

Improved Direct Torque Double Closed-Loop Control Algorithm for Induction Motor

Huaqiang ZHANG*, Tong YAO, Shijun LUO

Department of Electrical Engineering, Harbin Institute of Technology
Harbin 150001, China

*Corresponding author, e-mail: zhq@hit.edu.cn

Abstract

This paper presents an improved direct torque control (DTC) algorithm as compared to a traditional DTC scheme. In the traditional scheme, a pair of hysteresis comparators is used to control motor stator flux and electromagnetic torque. This causes a variable switching frequency which results in a high flux and torque ripples. To mitigate these issues, an improved DTC algorithm based on a double closed-loop is presented. Acting the induction motor as a control object, a mathematical model of the flux and torque based on proportional and integral (PI) controller in the double closed-loop is established. With the flux and the torque treated as control variables, a smooth and continuous vector control and a fast-response DTC are observed. By adopting this improved DTC algorithm, the simulation and experimental results indicate that the flux and the torque ripples reduced greatly. Additionally, the static and dynamic performances of the system are improved because of the mentioned scheme operating at a constant switching frequency.

Key words: direct torque control, double closed-loop, control algorithm, PI controller, torque ripple

Copyright © 2014 Institute of Advanced Engineering and Science. All rights reserved.

1. Introduction

Recently, the application of AC variable speed systems is becoming more extensive because of their simple structure, reliable operation, low price, and lack of commutation sparking and corrosion; further, it can be used in harsh environments.

The high-performance frequency controlled inverter for induction motor should be characterized by:

- 1) fast flux and torque response;
- 2) available maximum output torque in wide range of speed operation region;
- 3) constant switching frequency;
- 4) low flux and torque ripples;
- 5) robustness for parameter variation.

To improve the control performance of the induction motors in these systems, the control schemes of new induction motors are renewed constantly. Since the 1970s, vector control such as DTC and feedback linearization control has enabled the control performance of induction motors to be more favorable than that of DC motors. The DTC scheme in induction motors has a simpler structure, an increased robustness for parameter variation, and a better dynamic response to the torque. Therefore, DTC has received considerable attention from researchers [1].

In the traditional DTC control scheme, two hysteresis controllers are used to manipulate the stator flux and the torque of the motor. Because of the imperfection of the hysteresis controllers, torque ripples and variable switching frequencies still exist. To solve these problems, many new DTC strategies have been presented: the improved DTC scheme [2-5]; the dead-beat DTC scheme; a DTC scheme based on predictive flux control, torque control, and discrete space vector modulation; and schemes based on fuzzy logic and neural networks [6-8]. In this study, an improved DTC algorithm with flux and torque based on double closed-loop is investigated. Both simulation and experimental results indicate that this DTC scheme can greatly improve the control performance of the system.

2. Traditional DTC Scheme

In the traditional DTC scheme, the switching table determines the appropriate voltage vector to apply for direct flux and torque control, which results in errors when operating within a certain range [9]. The control theory diagram of the traditional DTC control scheme is shown in Figure 1.

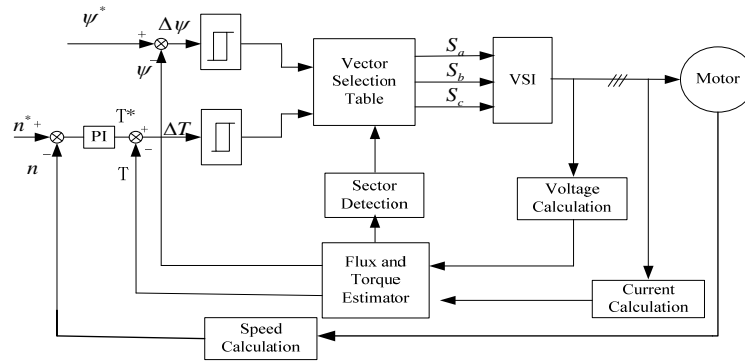


Figure 1. Control theory diagram of the traditional DTC scheme

The traditional DTC control scheme was established based on the induction motor model in a two-phase stationary $\alpha - \beta$ coordinate system. To accomplish this coordinate system, the voltage and the current are measured first. Then the current and voltage vectors are transformed from a three-phase stationary coordinate system to a two-phase.

The stator flux and the electromagnetic torque can be calculated according to induction motor mathematical model, and the flux sector can be determined with it. The calculated values of the stator flux and the electric torque are compared to their reference values; the errors are controlled by the hysteresis comparators. Then, the corresponding voltage space vector is selected based on both the error and sector signals which are controlled by the flux. The flux and torque errors are able to be maintained within the hysteresis band.

There are many ways to define the electromagnetic torque of the induction motor. In this paper, the electromagnetic torque equation is written as

$$T_e = \frac{m_s}{2} P_b \frac{L_m}{L_r L_s - L_m^2} \Psi_r \Psi_s \sin \gamma \quad (1)$$

where m_s is the number of power phases, P_b is the number of pole pairs, L_m is the mutual inductance, L_s is the stator inductance, L_r is the rotor inductance, Ψ_s is the stator flux amplitude, Ψ_r is the rotor flux amplitude, and γ is the angle between the rotor and stator flux vectors.

The electromagnetic torque can be altered by the relative angle between the stator flux and the rotor flux of the induction motor. The rotor flux is relatively static because it changes much slower than the stator flux. The above-mentioned angle can only be adjusted by altering the stator flux, which is controlled by the stator voltage. The stator flux in the $\alpha - \beta$ coordinate system can be expressed by

$$\Psi_s(t) = \int (\mathbf{u}_s(t) - \mathbf{i}_s(t) R_s) dt \quad (2)$$

where $\Psi_s(t)$ is the stator flux vector, $\mathbf{u}_s(t)$ is the stator voltage space vector, $\mathbf{i}_s(t)$ is the stator current space vector, and R_s is the stator resistance.

When the motor is operating at a high speed, the stator resistance is negligible. Then, Equation (2) can be written as

$$\mathbf{u}_s(t) \approx \frac{d\boldsymbol{\psi}_s(t)}{dt} \quad (3)$$

Equation (3) indicates that the stator flux change is related to the voltage vector, which is generated by an inverter. When the voltage vector is active in a period, the flux rotates along the direction of the voltage vector, creating a flux increment. As shown in Figure 2, when the stator flux is in the second sector, the voltage vectors U_3 and U_4 are active consecutively so that the flux vector amplitude rotates along a specific direction and is maintained within a range of the hysteresis controller.

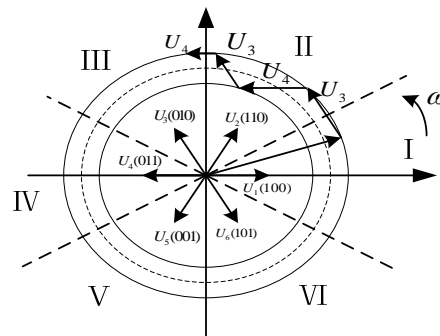


Figure 2. Stator flux track of traditional DTC scheme

Figure 2 shows that the stator flux amplitude ripples are controlled in the hysteresis band of the flux hysteresis controller and that the torque fluctuates with the flux. These ripples are caused by the hysteresis controller itself. To reduce these ripples radically, hysteresis control must be abandoned for an improved control algorithm.

3. Improved DTC Scheme

To reduce the torque ripples, a pair of PI regulators is used to control the stator flux and the magnetic torque instead of hysteresis controller. The steady state and dynamic performances are significantly improved by adopting PI controllers. The high flux and torque ripples caused by the hysteresis comparators are reduced, and the static error is eliminated [10-12].

To calculate the flux and torque errors accurately in every cycle, voltage space vector modulation technology is adopted [12-15]. It can be called the Direct Torque Control with Space Vector Modulation (DTC-SVM). The control theory diagram of the improved DTC algorithm is shown in Figure 3.

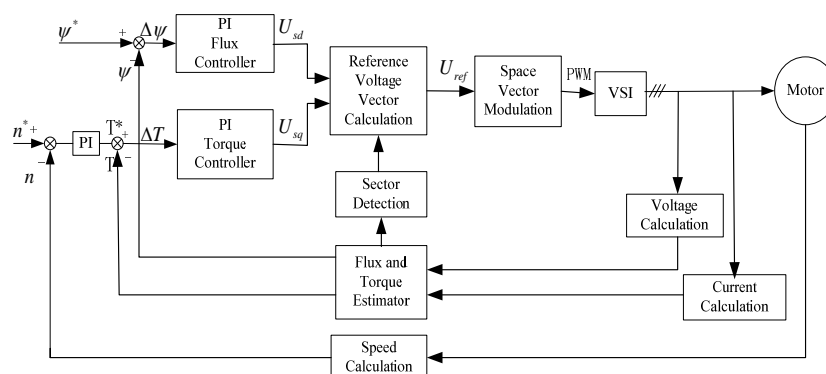


Figure 3. Control theory diagram of improved DTC algorithm

The required voltage vector that can exactly calculate the flux and torque errors is called a reference voltage vector (U_{ref}). Two PI controllers are used in this scheme to generate the reference voltage vector by adjusting the flux and torque. The improved DTC scheme is achieved in the stator flux coordinate system. The coordinate axes are expressed by d and q . The rotational speed of the coordinate axis is equal to the synchronization angular speed (ω_s) of the stator frequency. These parameters such as U_{sd} and U_{sq} are expressed in stationary d - q coordinates. The variables ψ and T play a key role in the design of the PI controller.

3.1. Mathematical Model of Induction Motor in Stator Flux Coordinates

The mathematical equation with the stator-flux-oriented induction motor is obtained by transforming the coordinates with respect to the equations of voltage, flux, and torque in the three-phase coordinate system [16], [17]. The coordinate system which rotates as the stator flux angular speed ω_s is called a d - q coordinate system. The induction motor mathematical equation in a d - q coordinate system is described as

$$\begin{cases} U_{sd} = R_s I_{sd} + p\psi_s \\ U_{sq} = R_s I_{sq} + \omega_s \psi_s \end{cases} \quad (4)$$

$$\begin{cases} 0 = R_r I_{rd} + p\psi_{rd} + \psi_{rq} (P_b \omega_m - \omega_s) \\ 0 = R_r I_{rq} + p\psi_{rq} + \psi_{rd} (\omega_s - P_b \omega_m) \end{cases} \quad (5)$$

where p is a differential divisor.
The flux is written as

$$\begin{cases} \psi_s = L_s I_{sd} + L_m I_{rd} \\ 0 = L_s I_{sq} + L_m I_{rq} \\ \psi_{rd} = L_r I_{rd} + L_m I_{sd} \\ \psi_{rq} = L_r I_{rq} + L_m I_{sq} \end{cases} \quad (6)$$

The torque and its motion equations are written as

$$\begin{cases} T_e = \frac{m_s}{2} P_b \psi_s I_{sq} \\ T_e - T_L = Jp\omega_m \end{cases} \quad (7)$$

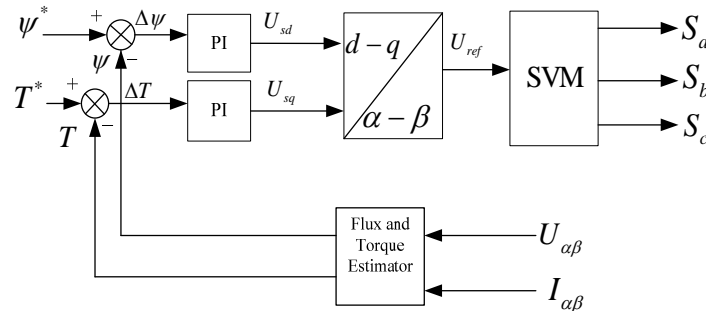


Figure 4. Improved DTC algorithm with stator-flux-oriented coordinate system

The improved DTC algorithm in a stator flux $d-q$ coordinate system is shown in Figure 4. The error signal $\Delta\psi$ is obtained by comparing the reference stator flux vector ψ^* with the estimated feedback value ψ . The output of the flux PI controller can be interpreted as the d -coordinate axis component (U_{sd}). The error signal ΔT is obtained by comparing the reference torque vector T^* with the estimated feedback value T . The output of the torque PI controller can be interpreted as the q -coordinate axis component (U_{sq}). The reference voltage vector U_{ref} is obtained by transforming these voltage vectors in the $d-q$ coordinate system into the $\alpha-\beta$ stationary coordinate system. The inverter can be driven by these switch signals, which are generated by space vector modulation.

3.2. PI Controller Design

The transfer function of the PI controllers is given as follows,

$$G_R(s) = \frac{U(s)}{E(s)} = K_p \left(1 + \frac{1}{sT_i} \right) \quad (8)$$

where K_p is the controller gain, T_i is the controller integrating time constant.

The PI controller diagram is shown in Figure 5.

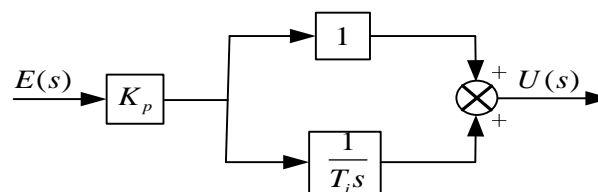


Figure 5. Diagram of PI controller

The above model of the controller was used in the improved DTC scheme with two PI controllers. The slip ratio can be neglected when the motor is operating at a high speed. The difference between the rotor speed and the synchronous speed is small, so $\omega_s - p_b\omega_m$ is nearly equal to zero. If the motor is not loaded, then $T_L = 0$. Therefore, the rotor speed can be expressed as

$$p\omega_m = \frac{1}{J} P_b \frac{m_s}{2} \psi_s I_{sq} \quad (9)$$

From Equation (7), I_{sq} is expressed as

$$I_{sq} = T_e \frac{2}{P_b m_s \psi_s} \quad (10)$$

The equations below can be obtained by using the voltage and flux equations of the induction motor in a $d-q$ coordinate system [7]

$$\begin{cases} (R_r L_s + \sigma L_s L_r p) U_{sd} \\ = [R_s R_r + p(R_r L_s + R_s L_r) + \sigma L_s L_r (p)^2] \psi_s \\ [(R_s L_r + R_r L_s) p + \sigma L_s L_r (p)^2] I_{sq} \\ = L_r p U_{sq} - L_r \psi_s P_b p \omega_m \end{cases} \quad (11)$$

Where $\sigma = 1 - \frac{L_m^2}{L_s L_r}$

The open-loop flux and torque transfer functions are defined as follows

$$\begin{cases} G_\psi(s) = \frac{\psi_s(s)}{U_{sd}(s)} \\ G_T(s) = \frac{T_e(s)}{U_{sq}(s)} \end{cases} \quad (12)$$

Where

$$\begin{aligned} \psi_s &= \frac{R_r}{\sigma L_r} + s; T_e = \frac{P_b m_s \psi_s}{2\sigma L_s} s; \\ U_{sd} &= s^2 + \frac{R_r L_s + R_s L_r}{\sigma L_s L_r} s + \frac{R_s R_r}{\sigma L_s L_r}; \\ U_{sq} &= s^2 + \frac{R_s L_r + R_r L_s}{\sigma L_s L_r} s + \frac{P_b^2 m_s \psi_s^2}{2\sigma L_s J} \end{aligned}$$

The flux and torque control loops are shown in Figure 6.

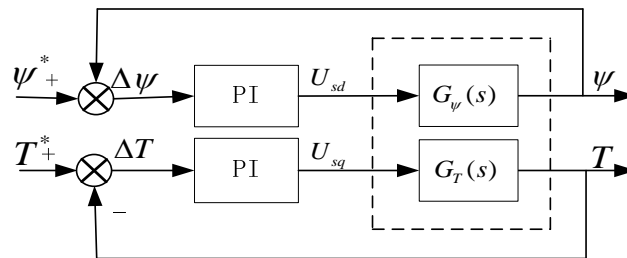


Figure 6. Block diagram of flux and torque control loop

The reference voltage vector U_{sd} in d coordinate axis is obtained via the PI controller by comparing the reference flux vector ψ_s^* with the feedback vector ψ_s . The reference voltage vector U_{sq} in q coordinate axis is obtained via the PI controller by comparing the reference torque vector T^* with the feedback vector T .

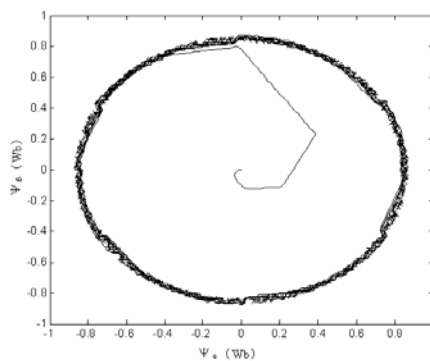
4. Analyses of Simulation and Experiment

To verify the advantages of the improved DTC algorithm, a simulation and an experiment were carried out. The parameters of the induction motor are listed in Table I. During the simulation, the reference stator flux amplitude is 0.85 Wb, the reference rotating speed is 1000 rpm, and the initial value of the reference load torque is zero. When $t = 0.004$ s, the load is 20 N·m. The switching frequency of the inverter is 10 kHz.

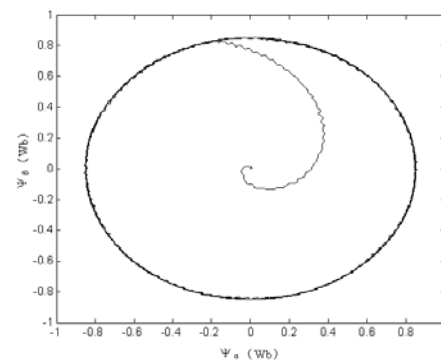
The results of the simulation and the experiment are shown in Figure 7–11. Figure 7 shows a stator flux track. In the improved DTC (DTC-SVM) scheme, the stator flux track is smoother than the traditional DTC. The electromagnetic torque waveform is shown in Figure 8. When the reference torque is 20 N·m, the torque ripple of the improved DTC scheme is reduced to 4%. Additionally, its ripple is smaller than the traditional scheme. The A phase current simulation waveform is shown in Figure 9. When $t = 0.05$ s, the motor works in steady state. Compared Figure 9.a) with Figure 9.b), the A phase current simulation waveform with the improved DTC is more smooth, and the current ripples are reduced.

Table 1. Parameters of Induction Motor.

Parameter	Value
Power	4 kW
Voltage	380 V
Frequency	50 Hz
Rated speed	1430 rpm
Stator winding resistance	1.405 Ω
Rotor winding resistance	1.395 Ω
Stator inductance	0.178 H
Rotor inductance	0.178 H
Mutual inductance	0.1722 H
Number of pole pairs	2
Moment of inertia	0.0131 kg·m ²

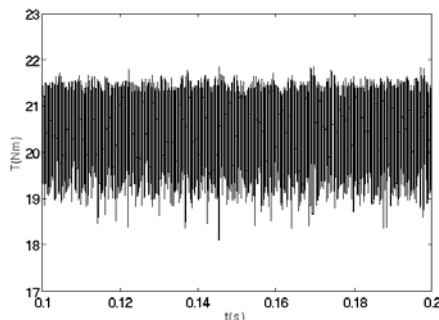


a) Simulation waveform of stator flux track with DTC

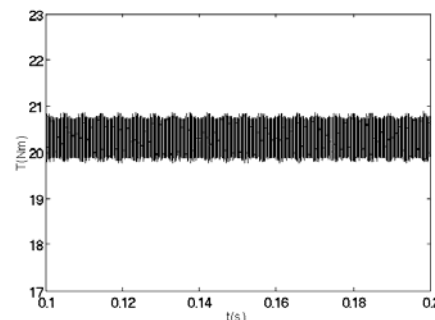


b) Simulation waveform of stator flux track with DTC-SVM

Figure 7. Simulation waveform of stator flux track



a) Torque simulation waveform with DTC



b) Torque simulation waveform with DTC-SVM

Figure 8. Torque simulation waveform in steady state

The experiment results, which are based on the TMS320LF2407 DSP platform, were analysed. A DC motor is used as a fictitious load. When the reference rotating speed was 1000 rpm, the load torque was 20 N·m, and the motor was operating stably, the torque and current waveforms were measured with an oscilloscope; the results are shown in Figure 10 and Figure 11. The results of the simulation and the experiment indicate that the improved algorithm is effective in reducing the torque ripples and in achieving a better performance in both dynamic and steady states.

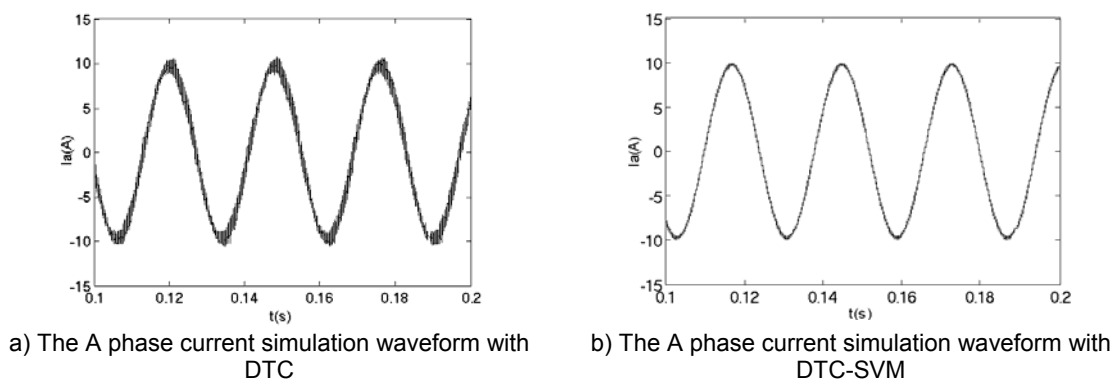


Figure 9. The A phase current simulation waveform in steady state

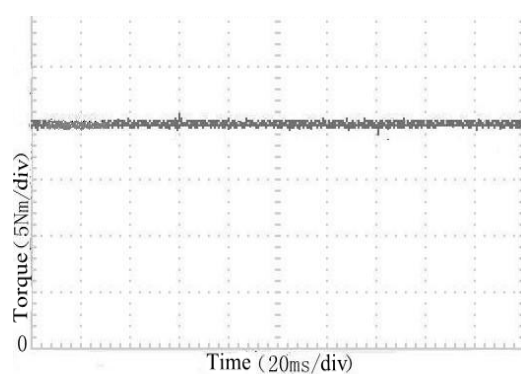


Figure 10. Torque experiment waveform in steady state

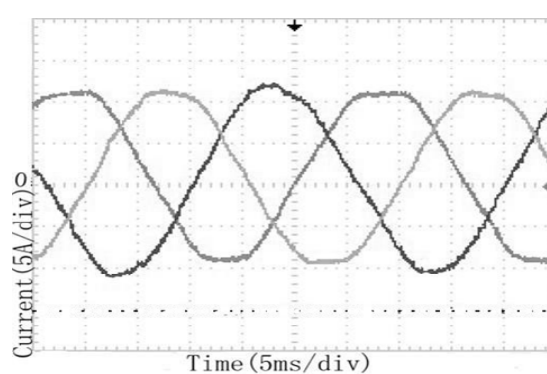


Figure 11. Phase current experiment waveform in steady state

5. Conclusion

To reduce the flux and torque ripples and maintain a constant switching frequency in the inverter, an improved DTC algorithm with flux and torque based on double closed-loop is presented. Acting the induction motor as a control object, the mathematical model of the flux and torque PI controller is established. With the flux and the torque treated as control variables, a smooth and continuous vector control and a fast-response are appeared in the improved DTC scheme. The traditional bang-bang control has been abandoned in this scheme, and a reference voltage vector is generated by the space vector modulation method to compensate for the flux error. The results from the simulations and the experiments indicate that the torque ripples are reduced to 4%, the flux and current fluctuations are significantly reduced, and the static and dynamic performances of the system are improved by the constant switching frequency of the improved DTC scheme.

References

- [1] L Tang, MF Rahman. *A new direct torque control strategy for flux and torque ripple reduction for induction motors drive by using space vector modulation*. 32nd Annual IEEE Power Electronics Specialists Conference. Vancouver, British Columbia. 2001; 3: 1440-1445.
- [2] Xuchao Huang, Rongwen Lin. *Novel design for direct torque control system of PMSM*. *TELKOMNIKA Indonesian Journal of Electrical Engineering*. 2013; 11(4): 2102-2109.
- [3] GS Buja, MP Kazmierkowski. *Direct torque control of PWM inverter-fed AC motors - a survey*. *IEEE Transactions on Industrial Electronics*. 2004; 51(4): 744-757.
- [4] Yaohua Li, Jingyu Liu, Jian Ma, Qiang Yu. *A Simplified voltage vector selection strategy for direct torque control*. *TELKOMNIKA Indonesian Journal of Electrical Engineering*. 2011; 9(3): 539-546.
- [5] K Qian, S Xie, M Gao. *Improved direct torque control method for induction motor applications*. *Journal of Chinese Electrical Engineering Science*. 2004; 24(7): 210-214.

-
- [6] D Casadei, F Profumo, G Serra, A Tani. FOC and DTC: two viable schemes for induction motors torque control. *IEEE Transactions on Power Electronics*. 2002; 17(5): 779-787.
- [7] G Xi, W Hu, S Yu. Fuzzy DSVM strategy in the direct torque control of an induction motor. *Electric Machines and Control*. 2006; 18(2): 435-449.
- [8] YC Zhang, JG Zhu. Direct Torque Control of Permanent Magnet Synchronous Motor With Reduced Torque Ripple and Commutation Frequency. *IEEE Transactions on Power Electronics*. 2001; 26(1): 235-248.
- [9] E Ozkop, HI Okumus. *Direct torque control of induction motor using space vector modulation (SVM-DTC)*. 12th International Middle East Power System Conference. Aswan, Egypt. 2008: 310-314.
- [10] M Zelechowski, MP. Kazmierkowski, F Blaabjerg. *Controller design for direct torque controlled space vector modulated (DTC-SVM) induction motor drives*. Proceedings of the IEEE International Symposium on Industrial Electronics. Dubrovnik, Croatia. 2005; 3: 951-956.
- [11] M Zelechowski, M Malinowski, P Kaczynski, W Kolomyjski, M Twerd, J Zaleski. *DSP-based sensorless direct torque control-space vector modulated (DTC-SVM) for inverter fed induction motor drives*. Problems of Automated Electrodrives Theory and Practice. Crimea, Ukraine. 2003: 90-92.
- [12] Y Zhu, V She, J Jiang. *Direct torque control based on symmetrical voltage vectors combination*. Proceedings of the CSEE. 2006; 26(23): 139-144.
- [13] HR Keyhani, MR Zolghadri, A Homaifar. *An extended and improved discrete space vector modulation direct torque control for induction motors*. 35th Annual IEEE Power Electronics Specialists Conference. 2004; 5: 3414-3420.
- [14] A Diaz, EG Strangas. *A novel wide range pulse width overmodulation method for voltage source inverters*. Applied Power Electronics Conference and Exposition, APEC2000, Fifteenth Annual IEEE. 2000; 1: 556-561.
- [15] Steimel. *Direct Self-Control and Synchronous Pulse Techniques for High-Power Traction Inverters in Comparison*. *IEEE Transactions on Industrial Electronics*. 2004; 51:810-820.
- [16] Jun Hu, Bin Wu. *New integration algorithms for estimating motor flux over a wide speed range*. *IEEE Transactions on Power Electronics*. 1988; 13(13): 969-977.
- [17] Hu Hu, Yong Dong Li, Yi Zeng. *Direct torque control of induction motor for railway traction in whole speed range*. IECON 02, Industrial Electronics Society, IEEE 2002 28th Annual Conference. 2002; 3: 2161-2166.